ANL-6582
Reactor Technology
(TID-4500, 17th Ed.)
AEC Research and
Development Report

ARGONNE NATIONAL LABORATORY
9700 South Cass Avenue
Argonne, Illinois

TWO SPHERICAL FAST CRITICAL EXPERIMENTS
(ZPR-III Assemblies 38 and 39)

by

J. C. Bates,* W. G. Davey,*
P. I. Amundson, J. M. Gasidlo,
J. K. Long, and W. P. Keeney

Idaho Division

July 1962

*Assigned to Argonne National Laboratory from the
United Kingdom Atomic Energy Authority

Operated by The University of Chicago
under
Contract W-31-109-eng-38

DISCLAIMER

TABLE OF CONTENTS

LIST OF FIGURES

LIST OF TABLES

TWO SPHERICAL FAST CRITICAL EXPERIMENTS (ZPR-III Assemblies 38 and 39)

by

J. C. Bates, W. G. Davey,
P. I. Amundson, J. M. Gasidlo,
J. K. Long, and W. P. Keeney

ABSTRACT

Two spherical versions of earlier cylindrical assemblies have been used for a critical study of shape effects for fast reactor cores with volumes of 300-400 liters. Assemblies 24 (cylindrical) and 38 (spherical) had a high-density metallic uranium blanket, whereas the set of assemblies numbered 31 (cylindrical) and 39 (spherical) had a low-density uranium-fueled core (with steel and aluminum diluents) with a high-density blanket of depleted uranium.

The main features of these assemblies are summarized below.

Assemblies		Density		Ratio of Length to Diameter for Cylinder	Volume of Sphere (liters)	Critical Mass of Sphere	Measured Shape Factor
Cylinder	Sphere	Core	Reflector				
24	38	High	High	0.927	298.7	424 kg	0.920 ± .003
31	39	Low	High	0.732	391.4	426.5	0.921 ± .002

Reactivity coefficients of a small number of fissile and nonfissile materials were measured in both assemblies (38 and 39). In Assembly 38 the effects of environment, etc., upon fission rates measured with absolute fission chambers were investigated.

Radial fission rate traverses in different directions were made in Assembly 39 to reveal any flux asymmetry due to heterogeneity of the core; no such effect was detected.

I. INTRODUCTION

Assemblies 38 and 39 were designed specifically to obtain shape factors appropriate to large cores diluted with U^{238} and with representative structural materials, respectively.

The shape factor of a reactor core is defined as the inverse of the ratio of its critical mass to the critical mass of a spherical reactor; the two reactors being compared must have identical core compositions and similar blanket parameters.

The investigations were prompted by some recent calculations of shape factors for fast reactors. These particular assemblies were chosen for their similarity to computed cases and thus to provide a direct check upon the accuracy. Care was taken to reproduce the same core composition as that of the corresponding cylindrical core, and to design as good a sphere as is practicable with the available materials.

Some reactivity coefficients and fission rate ratios were measured. Where possible, these were compared with values for the cylindrical versions, which must have had spectra closely similar to those of the corresponding spheres.

Other measurements included the effects of environment and of wall thickness of the fission chamber upon measured fission ratios, and fission rate traverses to detect asymmetry of flux distribution.

For the sake of clarity, Assemblies 38 and 39 have been treated independently.

II. DESCRIPTION OF ZPR-III

The ZPR-III assembly is a machine which is divided into halves, one fixed and the other movable. The principal feature of each half is a matrix consisting of a 31 x 31 array of stainless steel tubes, each 2.1755 in. high, 2.1835 in. wide, and 33.5 in. in depth. The neutron and gamma-ray detectors which drive the reactor instrumentation are located on top of each matrix. Five control rods enter each matrix from the rear. Figure 1 is a photograph of the machine. A complete description of the ZPR-III facility has been given by Cerutti et al.[1]

Reactor cores are simulated in ZPR-III by loading stainless steel drawers, containing core and blanket materials, into both matrices. Each core drawer contains the core materials in the desired proportions loaded to a length of half the core, so that each matrix contains half the core. The halves are then brought together to form the complete assembly.

In an assembly, the core drawers are not necessarily of the same composition, but may be of several types. In all cases, however, these are loaded in the matrix in a repetitive pattern called the unit cell.

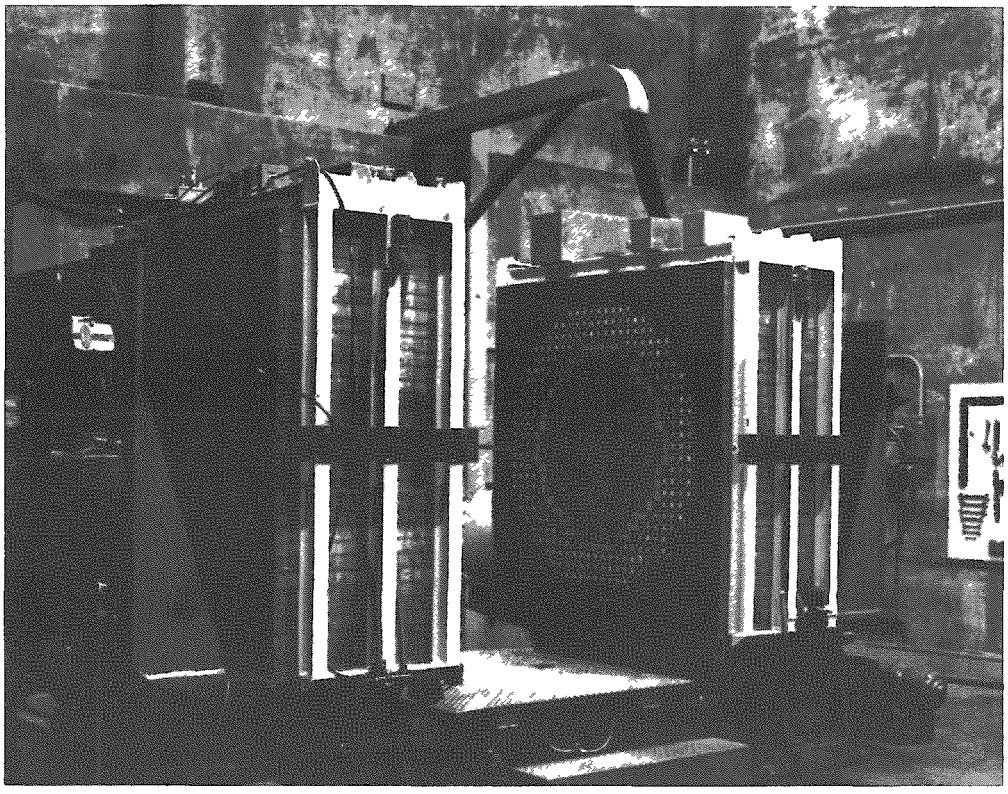

Fig. 1. The ZPR-III Critical Facility

III. ASSEMBLY 38, A SPHERICAL VERSION OF ASSEMBLY 24

A. Design of Assembly 24

Assembly 38 was designed to be as far as possible identical with Assembly 24 (see below), except that the core boundary was made "spherical" rather than "cylindrical," it being recognized that only approximations to these geometries can be built with the available materials. Because of this similarity it is advantageous to describe Assembly 24 fairly completely.

Assembly 24 was constructed with a five-drawer unit cell, there being eight $\frac{1}{8}$-in.-thick columns of 93% enriched uranium distributed through the 5 drawers. The only other material in the stainless steel drawers was depleted uranium as both core diluent and blanket. Figures 2 through 6 show schematic loading diagrams for the 5 basic drawers with the enriched columns made up of 2 x 2 x $\frac{1}{8}$-in. and 3 x 2 x $\frac{1}{8}$-in. pieces, and with the depleted uranium a variety of $\frac{1}{8}$-in.-thick plates and 1-in.-thick blocks. Although not shown in the figures, the enriched and depleted pieces were loaded in a specified pattern in each drawer, and this pattern was rigorously adhered to throughout the core.

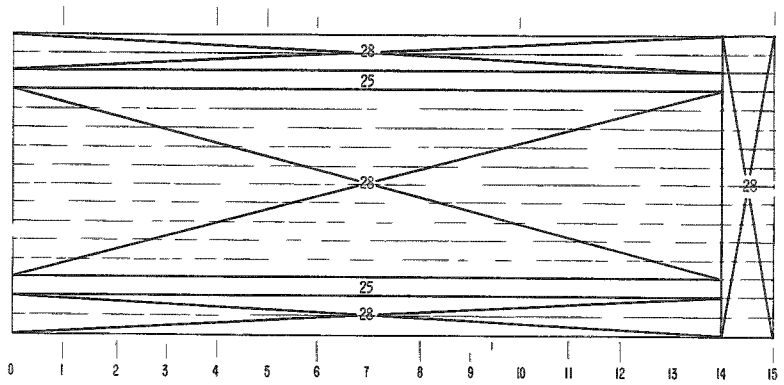

Fig. 2

Master No. 1,
Assembly 24

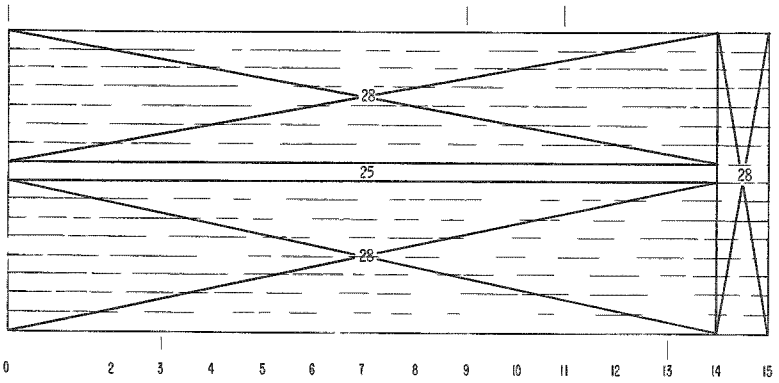

Fig. 3

Master No. 2,
Assembly 24

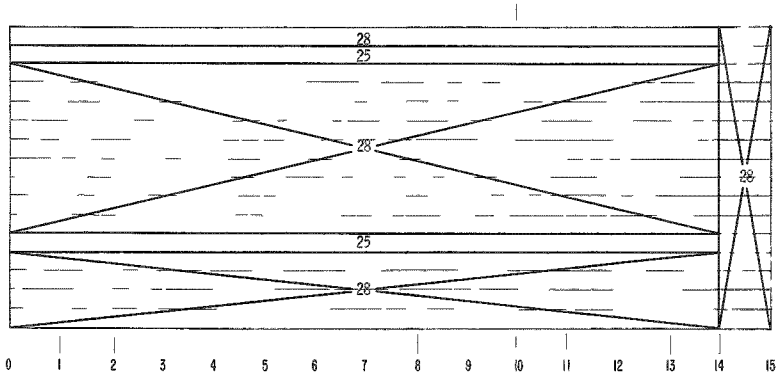

Fig. 4

Master No. 3,
Assembly 24

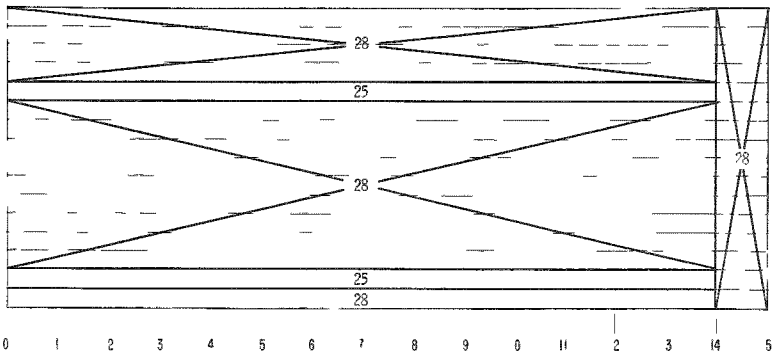

Fig. 5

Master No. 4,
Assembly 24

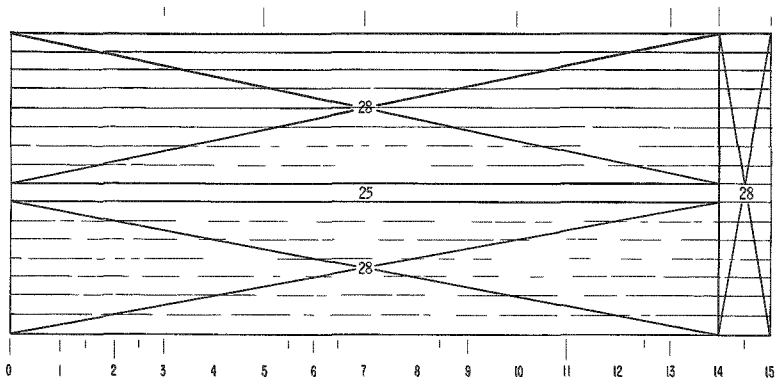

Fig. 6

Master No. 5,
Assembly 24

These drawers were loaded into the ZPR-III matrix tubes to form a pseudocylinder whose dimensions and composition are given in Table I.

Table I

ASSEMBLY 24 DATA

Core:

Material	Quantity (kg)	Volume Percent	Assumed Density of 100 v/o Material (g/cm^3)
U^{235}	460.7	7.57	18.75
U^{238}	4496.3	72.9	19.00
Stainless Steel	237.6	9.3	7.85

Blanket:

Material	Volume Percent	Assumed Density (g/cm^3)
U^{235}	0.19	18.75
U^{238}	83.30	19.00
Stainless Steel	7.31	7.85

Dimensions:

Core

Diameter (D)	76.88 cm (average)
Length (L)	71.27 cm
L/D	0.927

Blanket

Radial Thickness	33.7 cm (average)
Axial Thickness	30.5 cm

B. Design of Assembly 38

Assembly 24 most closely resembled Reactor 1 of the cases examined by Loewenstein and Main;[2] hence this case was used in the design of Assembly 38.

The calculations of Loewenstein and Main indicated that for the L/D of 0.927 for Assembly 24, the shape factor was 0.985; hence Assembly 38 should have had a critical U^{235} loading of 0.985 x 460.7 = 453.8 kg. At the U^{235} concentration of Assembly 24 (7.57 v/o at a density of 18.75 g/cm^3), this critical mass corresponds to a sphere of 42.42-cm (16.70-in.) radius. A pseudosphere of this radius was designed in layers of thickness equal to half the drawer height. In the region of the equator, the upper and lower halves of a drawer should have contained almost equal quantities of U^{235}, and in these instances they were made exactly equal. Near the poles of the sphere the upper and lower halves of a drawer contained different amounts of fuel.

In each layer, the drawer sequence that was used in Assembly 24 was reproduced exactly, except that the enriched uranium columns were terminated so that their ends lay on as perfect a circle as could be made with the available materials. The radii of these circles were determined so as to contain the correct quantity of U^{235}.

A comparison of the ideal U^{235} content of each layer (Fig. 7, layers H through X) and the mass obtained by the procedure outlined above is given in Table II. It can be seen that the desired mass in each layer was reproduced very accurately in the practical core design.

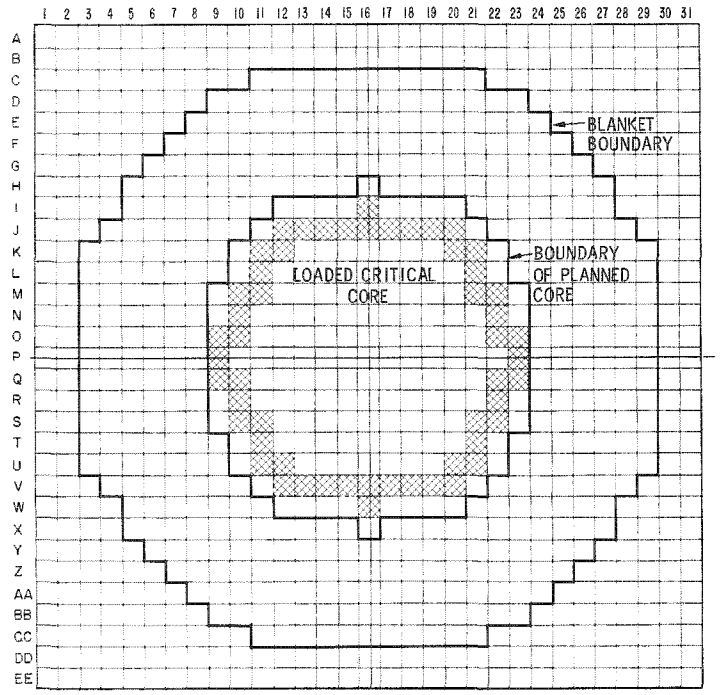

Fig. 7

Critical Loading of Assembly 38

Table II

IDEAL AND ACTUAL DESIGNED U^{235} MASSES[a] OF LAYERS OF DRAWERS IN ASSEMBLY 38

	Ideal U^{235} Mass (kg)		Designed U^{235} Mass (kg)	
Layers	Upper Half[b]	Lower Half[b]	Upper Half[b]	Lower Half[b]
H,X	-	0.18	-	0.17
I,W	2.39	5.02	2.39	5.06
J,V	7.47	9.73	7.45	9.74
K,U	11.78	13.68	11.84	13.65
L,T	15.37	16.87	16.13	16.13
M,S	18.20	19.30	18.77	18.77
N,R	20.25	21.00	20.60	20.60
O,Q	21.58	21.93	21.72	21.72
P	22.15	(c)	22.17	(c)
Mass in Core (sum x 2)	453.80		453.82	

(a) Including the U^{235} content of the depleted uranium.
(b) "Upper" and "Lower" refer to the distance from the equatorial P layer.
(c) The equator lies at the center of the P layer.

C. Approach to Criticality

The approach to critical was performed in the usual manner by adding drawers at the edge of the core. It was found that the system became critical at a loading of 426.7 kg of U^{235} with the control rod withdrawn 4.187 in. This is about 7% less than the designed loading; consequently, the critical core was not spherical. The vertical cross section at the interface of the halves is shown in Fig. 7 together with the outline of the planned core. It can be seen here that the main deviations from the design are the omissions at the poles of the sphere.

D. Edge Worth Measurements and the Critical Size of a Truly Spherical Assembly 38

1. Edge Worth Measurements

In order to estimate the critical size of a truly spherical Assembly 38, the effect of redistributing about 7% of the fuel at the edge of the assembly had to be determined. Accordingly, the edge worth of U^{235} was measured at 4 positions. In order to perform these measurements, the control rod was calibrated in the usual manner of determining the period corresponding to an incremental change of rod position. A computed

inhour curve was used to relate period to worth in inhours The inhour curve and the control rod calibration are given in Figs. 8 and 9 The positions at which the measurements were made are shown in Fig 10, and the results of the measurements are given in Table III

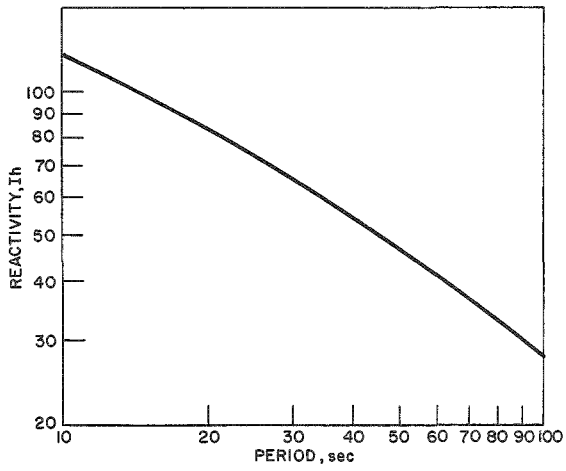

Fig. 8. Inhour Curve Used for Assemblies 24 and 38

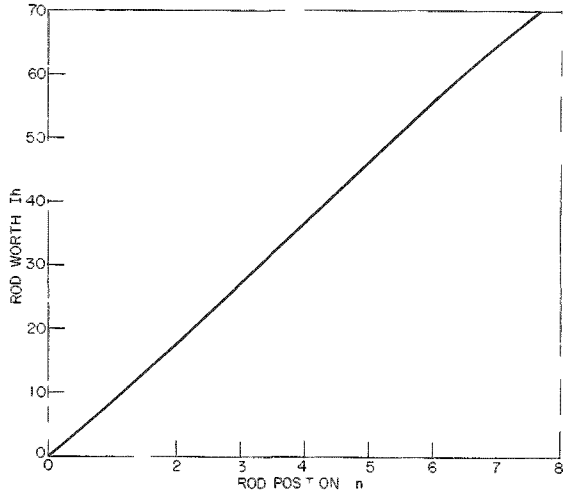

Fig 9. Control Rod Calibration Curve (Assembly 38)

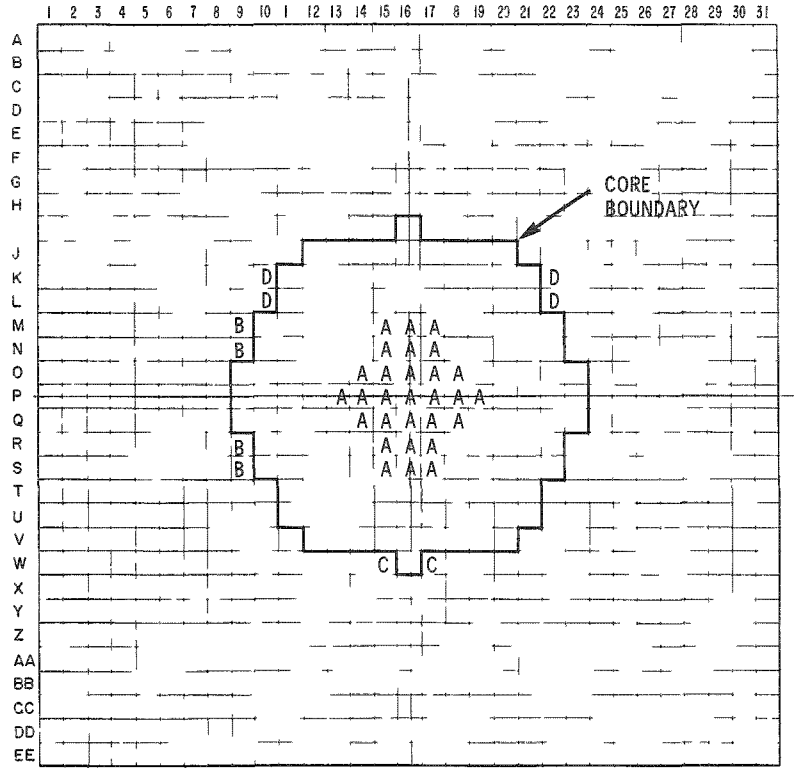

Fig. 10 Location of Edge Worth Measurements (Assembly 38)

Table III

EDGE WORTH OF U^{235}

Position (see Fig. 10)	Worth (Ih/kg U^{235})
A, End of Drawers, Equator	14.5
B, Side Drawers, Equator	13.1
C, Polar Cap	14.1
D, "Latitude 45°"	13.6

Table III shows that the edge worth of fuel does not vary greatly, which is to be expected, as the assembly is almost spherical. There is, however, a variation in worth of 0.7 about the mean value of 13.8 Ih/kg, and this must be reflected as an uncertainty in the critical mass of a true sphere.

2. Critical Mass of a True Sphere

The assembly was critical at a loading of 426.7 kg U^{235} with the control rod withdrawn 4.187 in. By means of the inhour curve of Fig. 8, this system was found to be 38.5 inhours supercritical. If the average fuel worth of 13.8 Ih/kg is used, then the assembly would be just critical at 423.9 kg of U^{235}.

Thus, the critical mass of the flattened sphere was 423.9 kg, and about 7% of edge fuel (i.e., about 453.8 - 423.9 $\approx$ 30 kg) must be redistributed to make the assembly spherical. This fuel is worth about the same amount at any point on the surface of the assembly, so that a true sphere would have a closely similar critical mass. However, there is an uncertainty of about 5% (i.e., 0.7 Ih/13.8 Ih) in the edge worth of the 30 kg U^{235}, and thus it is estimated that the critical mass of a truly spherical Assembly 38 is 424 $\pm$ 1.5 kg.

3. Shape Factor of Assembly 24

The critical mass of Assembly 24 was 460.7 kg, and thus the apparent shape factor for this assembly was (424 $\pm$ 1.5)/460.7, i.e., 0.920 $\pm$ 0.003.

It should be noted that although great care had been taken to make Assemblies 24 and 38 identical except in shape, uncertainties in, for example, the effects of roughness of the surface are not included in the above error.

E. Reactivity Coefficients in Assembly 38

Reactivity coefficients of a number of fissile and nonfissile samples were measured relative to void both at the center and near the edge of the assembly. At both positions, in the drawer in which the samples were placed and in the surrounding eight drawers, the $\frac{1}{8}$-in.-thick U^{235} plates in the first 6 in. were replaced by $\frac{1}{16}$-in. plates, thus homogenizing the region of measurement to some degree. The reactivity changes upon addition of the samples were obtained in the usual manner by noting the change of position of the control rod and by use of the calibration curve, Fig. 9.

The results are presented in Table IV. In all cases corrections for the presence of materials other than the principal ones have been made.

Table IV

A. CENTRAL REACTIVITY COEFFICIENTS (P-16 DRAWERS)[a]

Sample	(Ih/kg)
U^{233}	296 ± 5
U^{235}	164 ± 2
Pu^{239}	289 ± 3
S	-19 ± 3
W	-14.4 ± 0.3
Th	-16.0 ± 0.3

B. EDGE REACTIVITY COEFFICIENTS (P-10 DRAWERS)[a]

S	2.0 ± 2.5
W	-0.6 ± 0.3
Th	-0.9 ± 0.3
Stainless Steel	1.9 ± 0.5

[a]See Fig. 7 for the position of these drawers.

In all cases the error is assumed to be due solely to the ±0.5-Ih uncertainty arising from opening and closing the halves of the machine to insert the samples.

The central reactivity coefficients of all these materials (with the exception of tungsten) were also measured in Assembly 24. The results from both assemblies were in general agreement.

F. Central Fission Ratios

A series of absolute fission chamber measurements were made at the center of Assembly 38 to examine (1) repeatability of measurements, (2) effects of chamber design, and (3) effects of the local environment.

1. Repeatability of Measurements

The core compositions of Assemblies 24 and 38 are identical and the core sizes are similar; therefore, the central spectra and central fission ratios should be similar. Hence, the repeatability of measurements obtained with the Kirn absolute fission chambers could be checked by comparison of the central fission ratios in the 2 assemblies. Four such comparisons were made, the operating conditions of the chambers being determined in the usual manner by measuring their voltage and bias plateaus. The same chambers that were used in Assembly 24 were also used in Assembly 38, in order to minimize uncertainties in the comparison. The ratios were measured with the chambers in their usual positions at the fronts of the central drawers (1-P-16 and 2-P-16), and the single $\frac{1}{8}$-in.-thick fuel column in these drawers was replaced by two $\frac{1}{16}$-in.-thick columns placed one on each side of the chamber cables. The fuel arrangements in the surrounding drawers were not altered.

The results of the comparisons are given in Table V, the errors quoted being one standard deviation and derived from the counting statistics only.

Table V

REPEATABILITY OF KIRN FISSION CHAMBER MEASUREMENTS

Fission Ratio	In Assembly 24	In Assembly 38	Assy. 38 Value / Assy. 24 Value
$\frac{Pu^{239}}{U^{235}}$	1.14 ± 1%	1.17 ± 1%	1.03 ± 0.015
$\frac{U^{233}}{U^{235}}$	1.44 ± 1%	1.44 ± 1%	1.00 ± 0.015
$\frac{U^{234}}{U^{235}}$	0.246 ± 1%	0.268 ± 1%	1.09 ± 0.015
$\frac{U^{238}}{U^{235}}$	0.0284 ± 1%	0.0308 ± 1%	1.08 ± 0.015

It is clear from these data that the repeatability of the Kirn fission chamber measurements can be much worse than the counting statistics. The fact that all the Assembly 38 values are equal to or larger than those in Assembly 24 suggests that the U^{235} data were suspect in one or both of the assemblies, but the 2 sets of data cannot be brought into agreement by assuming that only one chamber gives erroneous data. Hence, it must be concluded that at least some of the fission ratios measured with the Kirn fission chambers may be in error by up to 9%, and that at present it is probably necessary to assume that all the measured ratios are uncertain to something less than this value.

2. Some Effects of Chamber Design on Measured Fission Ratios

Davey and Curran[3] have shown that measurements of the fission ratios of threshold materials in fast spectra are affected by the thickness of the steel walls of the chambers and by the proximity of the cables used with them. The measured changes are in rough agreement with those predicted on the basis of inelastic scattering in the chamber walls, and it appears that this scattering and the moderation occurring due to the presence of hydrogenous material in the cable can cause changes of the order of 5%.

In order to evaluate these effects in ZPR-III assemblies, 2 types of fission chambers were used. One of these was essentially identical with the Kirn chambers in all dimensions (in particular it possessed fairly thick walls) and differed only in that the fissile foil is removable and that it is a gas-flow chamber. The other type of chamber was also a gas-flow chamber from which the fissile foil could be removed. The external dimensions were closely similar to the heavy-walled chamber and the Kirn chamber except for the addition of a metallic extension to the connector, so that the cable was removed 2 in. further from the fissile material. The walls of the chamber, however, were very much thinner than in the other types, and scattering in these walls should be trivial.

Comparison of a fission ratio measured with thick- and thin-walled gas-flow counters gives a measure of the moderating effects of both wall and cable. The effect of the cable alone was estimated by obtaining ratios with the Kirn counters with and without an additional 3 in. of cable laid behind the counters. The results of these measurements are given in Table VI. In all these measurements the $\frac{1}{8}$-in. fuel column in the center drawer was replaced by two $\frac{1}{16}$-in. fuel columns placed one on each side of the chamber cable. In all cases the (one standard deviation) counting error was 1%.

Comparison of Experiments 1 and 2, and of 3 and 4, shows that in Assembly 38 the cable did not significantly affect the U^{234}/U^{235} or U^{238}/U^{235} fission ratios.

Comparison of Experiments 1 and 5 shows that the Kirn chambers and the thick-walled gas-flow chambers gave the same U^{238}/U^{235} ratio.

Comparison of Experiments 5 and 6 shows that the U^{238}/U^{235} fission ratio was decreased by $7\frac{1}{2} \pm 1\frac{1}{2}$% by the use of thick-walled chambers. This result is in reasonable agreement with that obtained by Hess et al. in ZPR-III Assembly 35, and it therefore appears probable that all U^{238}/U^{235} ratios measured with Kirn chambers in ZPR-III assemblies were about 7% to 8% too low due to inelastic scattering in the chamber walls.

Table VI

EFFECTS OF WALL THICKNESS AND CABLE ON MEASURED FISSION RATIOS

Chamber	Expt	Additional 3 in of Cable	Ratio
Kirn	1	No	$\frac{U^{238}}{U^{235}}$ 0.0308 ± 0 0003
Kirn	2	Yes	$\frac{U^{238}}{U^{235}}$ 0.0308 ± 0 0003
Kirn	3	No	$\frac{U^{234}}{U^{235}}$ 0.268 ± 0.003
Kirn	4	Yes	$\frac{U^{234}}{U^{235}}$ 0.264 ± 0.003
Thick-wall Gas Flow	5	No	$\frac{U^{238}}{U^{235}}$ 0 0312 ± 0.0003
Thin-wall Gas Flow	6	No	$\frac{U^{238}}{U^{235}}$ 0.0335 + 0.0003

It should be noted that this type of error will be present not only in the Kirn chamber measurements of the U^{238}/U^{235} ratio, but also in all such measurements involving threshold fissionable materials (see Davey and Curran[3] for estimates of these effects)

A further point of interest is that the thin-walled gas-flow U^{238}/U^{235} ratio of 0.0312 is 18% higher than the value of 0 0284 obtained with Kirn chambers in Assembly 24 (see Table V)

3. Some Effects of the Local Environment upon Measured U^{238}/U^{235} Fission Ratios

It is always necessary to remove some core material in order to insert fission chambers, and frequently this necessitates the movement of fuel within the drawers containing the chambers Usually, the $\frac{1}{8}$-in. fuel in these drawers is replaced with $\frac{1}{16}$-in fuel (i.e , the drawer is homogenized to some extent), and on occasion this homogenization is also carried out in the drawers surrounding the chambers.

In the present assembly, an attempt was made to assess the magnitude of the changes in the U^{238}/U^{235} ratio caused by redistribution of fuel in the vicinity of the chambers, as it was believed that this would give a measure of the validity of such measurements with fission chambers.

The results of these preliminary measurements are presented in Table VII. Included in Table VII are some relevant data which have already been quoted in Table VI. The errors in all cases (one standard deviation) are 1%.

Table VII

SOME EFFECTS OF LOCAL ENVIRONMENT ON THE MEASURED U^{238}/U^{235} FISSION RATIO

Case	Fuel Arrangement[a]	Chamber	U^{238}/U^{235} Ratio
1	2 x $\frac{1}{16}$-in. plates symmetrical in center drawers	Kirn	0.0308
2	2 x $\frac{1}{16}$-in. plates symmetrical in center drawers	Thin-walled gas flow	0.0335
3	2 x $\frac{1}{16}$-in. plates both on one side of center drawers	Kirn	0.0318
4	2 x $\frac{1}{16}$-in. plates both on one side of center drawers	Thin-walled gas flow	0.0352
5	4 x $\frac{1}{16}$-in. plates in center drawers: 9 central drawers homogenized	Kirn	0.0309
6	2 x $\frac{1}{8}$-in. plates in center drawers: 9 central drawers homogenized	Kirn	0.0307

[a] In the first 4 cases, the fuel was rearranged only in the central drawers.

Cases 1 and 2, and 3 and 4, show that the U^{238}/U^{235} ratio was changed by 3% to 5% by placing the fuel asymmetrically in the center drawers.

Case 1, 5, and 6 show that the U^{238}/U^{235} ratio does not apparently depend upon the number of drawers homogenized or alter when the amount of fuel in the central drawer is doubled.

It must be emphasized that these data are preliminary, and it is inadvisable at present to assume these effects are present in all assemblies, but only to recognize that some fission ratios may be slightly affected by the local environment.

G. Summary of Conclusions

1. The critical mass of Assembly 38 was 424 ± 1.5 kg U^{235}. The shape factor for Assembly 24 was thus 424/460.7 = 0.920 ± 0.003.

2. The central reactivity coefficients of a number of materials were in reasonable agreement for Assemblies 24 and 38.

3. The repeatability of measurements with the Kirn fission chamber was appreciably worse than the statistical accuracy and may be no better than about ±5%.

4. The chamber cable did not significantly affect the U^{234}/U^{235} and U^{238}/U^{235} fission ratios.

5. Kirn chamber measurements of the U^{238}/U^{235} fission ratio were about 7% too low due to inelastic scattering in the chamber walls.

6. Some appreciable changes in the fuel arrangement near the fission chambers did not affect the measured U^{238}/U^{235} fission ratio, but this was altered by about 4% when the fuel loading in the center drawers was asymmetric.

IV. ASSEMBLY 39, A SPHERICAL VERSION OF ASSEMBLY 31

A. Design of Assembly 31

The unit cell of Assembly 31[4] consisted of 5 columns of enriched uranium and 7 columns of depleted uranium uniformly distributed across a horizontal sequence of 4 drawers (see Fig. 11). Thus, the fuel plates were located in different positions in each drawer, and one drawer contained 2 columns of fuel. Because of this uneven distribution of the fuel plates, the drawers were loaded into the matrix so that any given column of the matrix always contained the same type of drawer. Thus, the columns of fuel within the drawers lined up to form large columns of fuel throughout the matrix. This is the usual arrangement of fuel plates in ZPR-III assemblies.

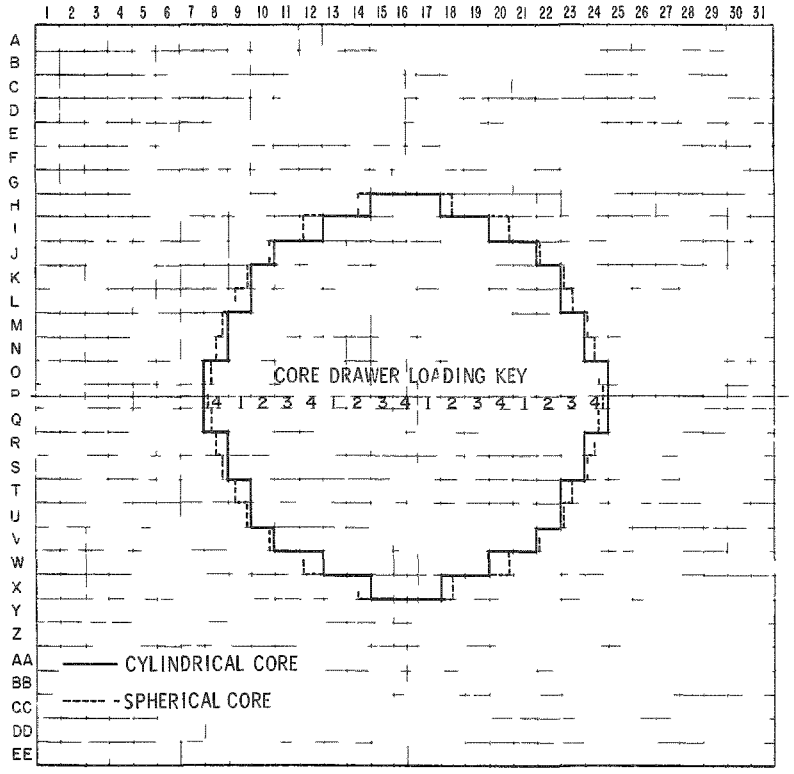

Fig. 11. Core Outlines (Assemblies 31 and 39)

The other core materials in the unit cell were the same for each drawer and consisted of 3 columns of stainless steel, 9 columns of 45%-density aluminum, and one column of 63%-density aluminum. The arrangement of the materials in the 4-drawer sequence is shown in Figs. 12-15.

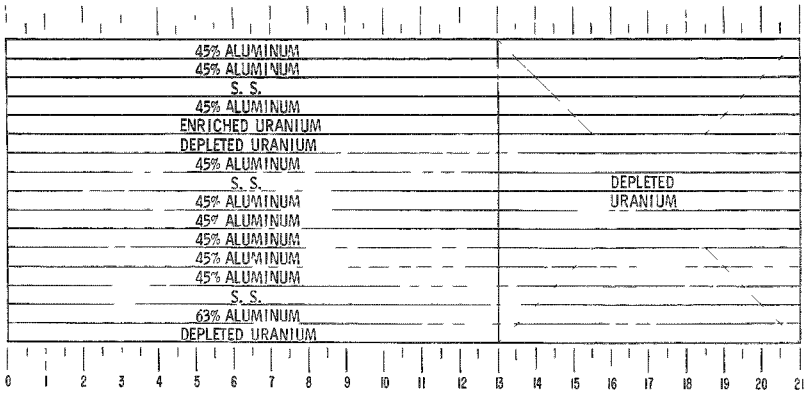

Fig. 12. Master No. 1, Assembly 31

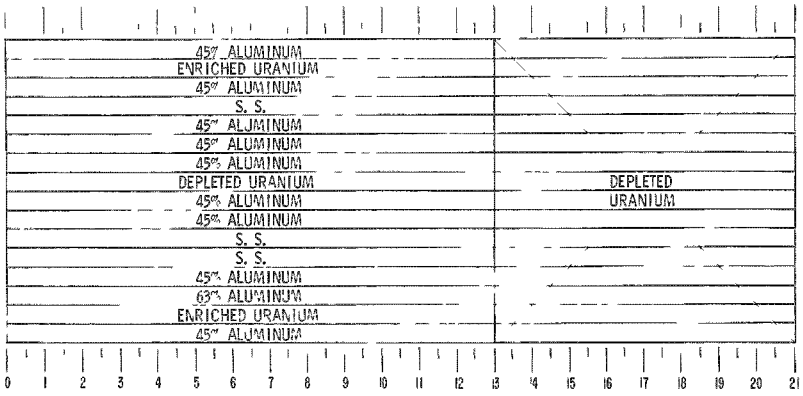

Fig. 13. Master No. 2, Assembly 31

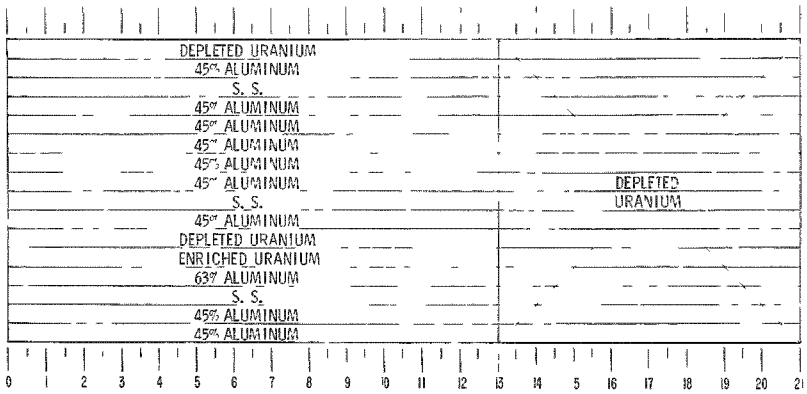

Fig. 14. Master No. 3, Assembly 31

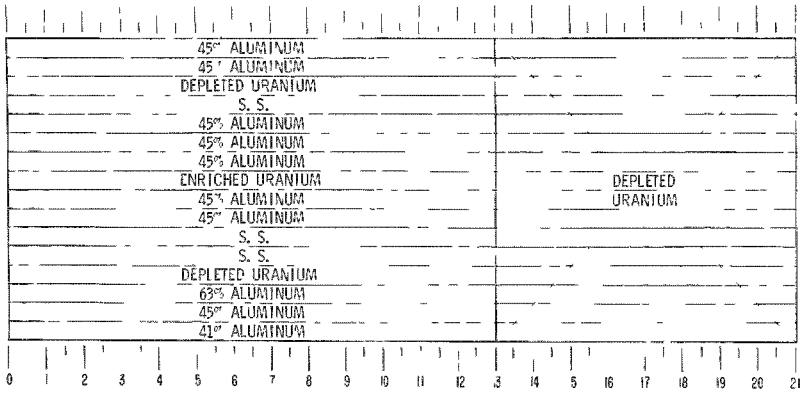

Fig. 15. Master No. 4, Assembly 31

The parameters of the critical core are given in Table VIII.

Table VIII

PARAMETERS OF THE CRITICAL CORE
(Assembly 31)

Material	Total Mass (kg)	Assumed Density, g/cm^3	Volume Fractions		
			Unit Cell	Critical Core	Blanket
U^{235}	463.1	18.75	0.05812	0.0581	0.19
U^{238}	738.4	19.00	0.09139	0.0914	83.30
Stainless Steel	818.4	7.85	0.2447	0.2453	7.31
Aluminum	269.6	2.70	0.2333	0.2349	-

Core Dimensions:

Height	66.2 cm
Radius	45.2 cm
Volume	425.0 liters
Axial Blanket	33.0 cm
Radial Blanket	27.5 cm

The differences between the volume fractions of the critical core and the unit cell were caused by unequal utilization of the 4 types of drawers; 54 drawers containing 2 x 13-in. stainless steel pieces and one 1-in. and four 3-in.-long pieces of enriched uranium.

B. Design of Assembly 39

Assembly 39 was designed on the basis of a shape factor of 0.92, calculated by Loewenstein and Main[2] for a reactor similar to Assembly 31. The planned critical mass of Assembly 39 was therefore 426.1 kg U^{235}.

The desired spherical core was approximated by a series of discs of thickness equal to the 2-in. depth of a matrix cell (see Fig. 11). The volume and U^{235} content of each disc equalled that of the corresponding part of the equivalent, perfectly spherical core. The edges of the discs were made as circular as possible by means of $\frac{1}{8}$ x 2 x $\frac{1}{2}$-in. fuel and diluent pieces.

The core materials were loaded following as closely as possible the 4 basic drawer loadings used in Assembly 31 (see Figs. 12-15); the fuel and diluent columns were lengthened or shortened as necessary. The type of drawer loading used in each column of Assemblies 31 and 39 are shown in Fig. 11. As in Assembly 31, a number of drawers (54) containing 2 x 13-in. stainless steel pieces (and mainly 3-in.-long fuel pieces) were distributed through the core (see Fig. 16).

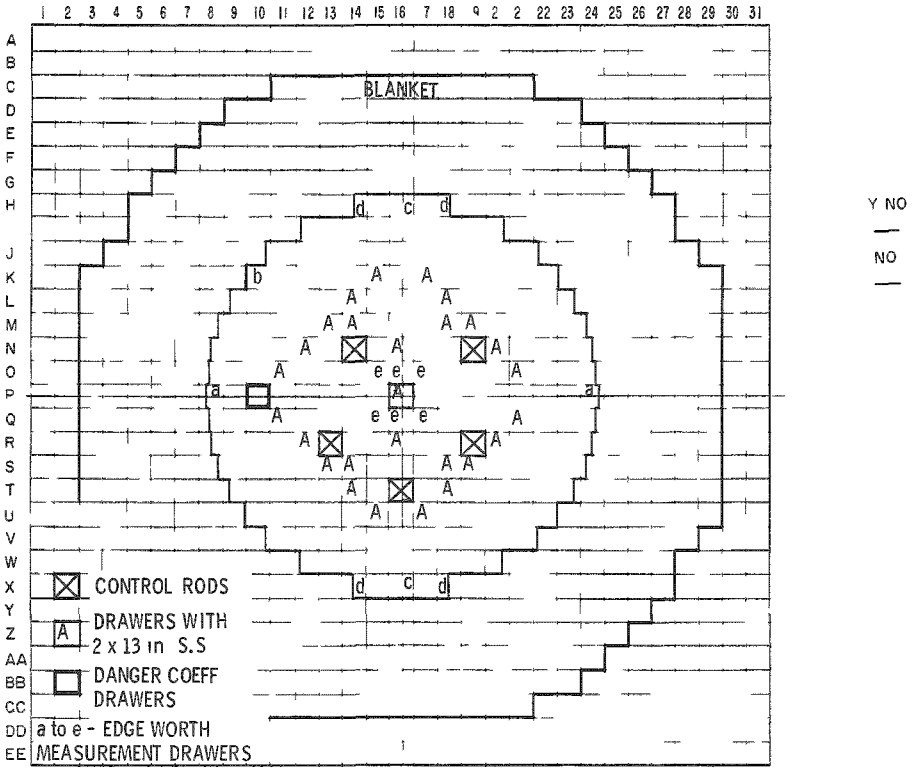

Fig. 16. Position of Drawers Used in Edgeworth Measurements, etc.; Half No. 1 (Assembly 39).

Assembly 31 had depleted uranium axial and radial blankets, 13 and 11 in. thick, respectively; the blanket of Assembly 39 was 12 in. thick.

Table IX compares the actual and ideal U^{235} loadings in each layer of the core, as originally planned (this core was very slightly subcritical).

Table IX

IDEAL AND ACTUAL MASSES OF U^{235} IN LAYERS OF THE CORE
(As Originally Planned)

Layer	g of U^{235}	
	Ideal	Actual
H, X	2.313	2.306
I, W	10.570	10.557
J, V	18.077	18.061
K, U	24.428	24.407
L, T	29.629	29.654
M, S	33.669	33.785
N, R	36.554	36.558
O, Q	38.292	38.297
P	38.863	38.876

Total for Core - 426.1 kg

Details of the critical core are given in Table X below:

Table X

PARAMETERS OF THE CRITICAL CORE
(Assembly 39)

Material	Total Mass (kg)	Assumed Density (g/cm^3)	Volume Fractions		
			Assembly 39	Assembly 31	Blanket
U^{235}	426.5	18.75	0.0581	(0.0581)	0.19
U^{238}	674.3	19.00	0.091[a]	(0.0914)	83.30
Stainless Steel	754.0	7.85	0.245	(0.245)	7.31
Aluminum	247.3	2.70	0.234	(0.235)	-
Core Dimensions:					
			Radius	45.4 cm	
			Volume	391.4 liters	
			Blanket	30 cm	

[a] Approximate figure; the columns of depleted uranium continue into the blanket.

C. Approach to Critical and Critical Mass

Additions to the core were made by replacing depleted uranium with core material at the edge of the existing core. With the planned loading of 426.1 kg U^{235} in place, the approach curves indicated a critical mass of 426.7 kg (see Fig. 17). The reactor was made critical with a loading of 429.3 kg and control rod No. 10 withdrawn 7.100 in. The BF_3 counters used during the approach to critical and the neutron sources were then moved away from the core and the spaces filled with blanket material. The critical position of rod No. 10 was 7.524 in. and the critical mass of the fully blanketed core was estimated as 426.5 kg U^{235}.

D. Control Rod Calibration

Measurements were made to find the stable reactor period corresponding to a measured movement of the control rod from a balance position. The relationship between period and reactivity was that used for Assembly 31 and is shown in Fig. 18. The period was kept within acceptable limits by moving rod No. 1.

The calibration curve for rod No. 10 is shown in Fig. 19.

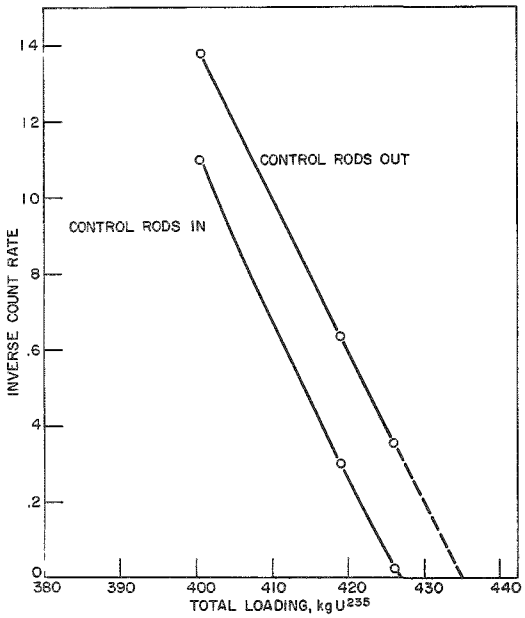

Fig. 17. Inverse Subcritical Count Rate versus Total Mass of U^{235} (Assembly 39).

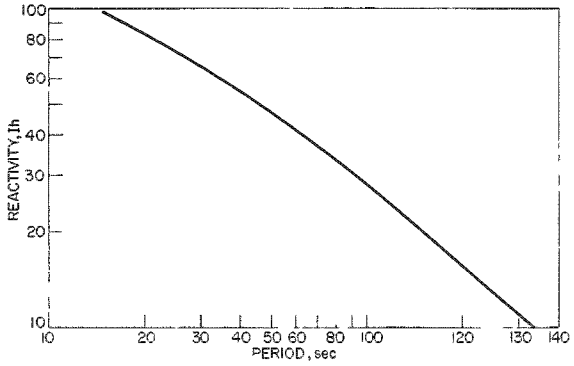

Fig. 18. Inhour Curve Used for Assemblies 31 and 39

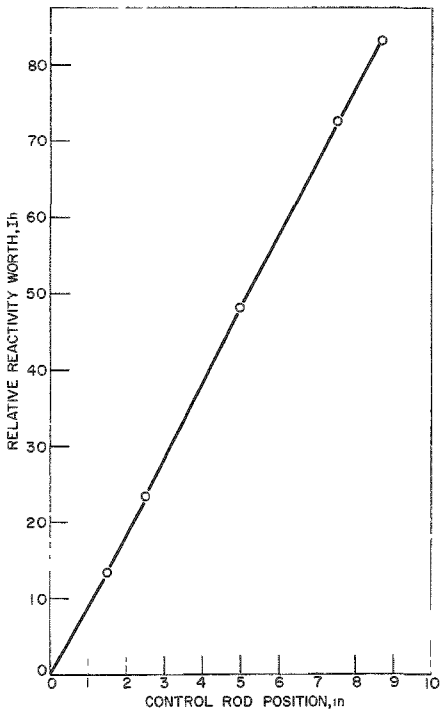

Fig. 19. Control Rod Calibration Curve, Rod No. 10, Assembly 39

E. The Reactivity Worth of Core Edge Material

The worth of core material relative to blanket material at the edge of the core was measured by replacing various core drawers with depleted uranium and finding the change in critical position of rod No. 10.

The drawers involved, the mass of U^{235} involved, the loss of reactivity, and the loss of reactivity per kg U^{235} are given in Table XI. Figure 16 shows the positions of the drawers involved.

Table XI

REACTIVITY WORTH OF CORE EDGE MATERIAL

Drawers Replaced	Mass of U^{235} Removed (kg)	Loss of Reactivity, (Ih)	Ih/kg
P-8 and P-24, both halves	0.937	22.2 ± 0.5	23.7 ± 0.5
1-K-10 and 2-K-22	1.274	35.2	27.6 ± 0.4
H-16 and X-16, both halves	1.074	23.7	22.1 ± 0.5
H-14 and X-14, both halves H-18 and X-18, Half No. 1	1.002	23.2	23.2 ± 0.5
O and Q-15, 16 and 17,[a] Half No. 1	0.934	28.4	30.4 ± 0.5
		Average =	25.4

[a] Core material was removed from the rear of these drawers; 2 in. from O and Q-16 and $2\frac{1}{2}$ in. from O and Q-15 and 17.

The spread of the results is attributed to:

1. differences in the mean distance from the core center of the material involved;
2. the varying amount and composition of the core diluents removed along with the U^{235}; and
3. the core not being truly spherical.

Since the estimate of critical mass was made from subcritical data, the accuracy of the edge-worth measurement is unimportant as regards the former; however, the critical mass, obtained from the first supercritical loading data and the average edge-worth value, is 426.3 kg, 0.05% lower than obtained from the approach curves.

A lower value for edge worth was obtained for Assembly 31 (18 Ih/kg), as the value quoted was a mean value for the whole length of the cylindrical core.

F. Effect of "Stepwise" Construction of the Core

Due to the differences in diameter of the cylindrically shaped layers comprising the core, there are "steps" in the core surface. The effect of changing the size of these steps at one of the "polar caps" was measured. The radii of the various cylindrical layers of core material are given in Table XII; in the upper two layers the 2-in. steps were replaced by 1-in. steps.

Table XII

RADII OF THE VARIOUS LAYERS OF THE CORE

Row	Original Radius, (in.)	Radius after "Smoothing", (in.)
H	4.35	H upper, 1.83 H lower, 5.88
I	9.31	I upper, 8.3 I lower, 10.16
J	12.17	
K	14.15	
L	15.58	
M	16.61	
N	17.31	
O	17.72	
P	17.85	

The change was made without altering the total mass of fuel involved.

The reactivity increase was 9.8 ± 0.5 Ih, equivalent to 0.1% of the critical mass.

G. Shape Factor of Assembly 31

The critical mass of Assembly 39, uncorrected for heterogeneity, separation of the halves, and "stepwise" construction, was found to be 426.5 kg U^{235}. The corresponding mass for Assembly 31 was 463.1 kg. The major uncertainty in a shape factor for Assembly 31, derived from these masses, is expected to be due to the differing degrees to which the cores approximate a cylinder and a sphere. (The outlines of the cores are compared in Fig. 11.)

A purely subjective estimate of "roughness" indicates that it is about the same for both cores. In view of the small effect of smoothing a "polar cap" of the spherical core, it is believed that the shape factor for a truly cylindrical version of Assembly 31 has been determined within ≈0.2% and that the shape factor is 0.921 ± 0.002.

H. Reactivity Coefficient Measurements

Substitutions were made at the core center and near the core edge (at a radius of 13.1 in.). The positions of the substitutions are shown in Fig. 16.

The samples of materials of low reactivity were 8 $in.^3$ in volume, whereas those of U^{235}, Pu^{239}, and polyethylene were small.

The samples were loaded as for Assembly 31[4] and results for the samples are relative to void.

Results for U^{235} and Pu^{239} at the core center agreed, within experimental error, with results for Assembly 31 (see Table XIII), although reactivity coefficients for these isotopes are not sensitive to spectra.

Table XIII

COMPARISON OF CENTRAL REACTIVITY COEFFICIENTS OF FISSIONABLE MATERIALS FOR ASSEMBLIES 31 AND 39

Material	Sample Mass, (kg)	Worth (Ih ± 0.5)	
		Assembly 31	Assembly 39
Enriched U (93.1%)	0.2878	29.0	29.0
Pu^{239} Mixture(a)	0.1860	34.0	35.0
		Worth (Ih/kg)	
		Assembly 31	Assembly 39
U^{235}		108 ± 1.9	108 ± 1.9
Pu^{239} (a)		192 ± 2.8	197 ± 2.8

(a) The isotopic concentrations were 94.51% Pu^{239}, 5.11% Pu^{240}, and 0.38% Pu^{241}. The isotopic value for Pu^{239} was calculated on the assumption that the Pu^{240} has $\frac{1}{5}$ of the worth of Pu^{239}.

Results for substitutions at the core center and near the core edge are given in Tables XIII through XV. Errors are based on an assumed uncertainty of ±0.5 Ih resulting from opening and closing the halves to change samples.

Table XIV

CENTRAL REACTIVITY COEFFICIENTS OF NONFISSILE MATERIALS
(Assembly 39)

Material	Sample Mass, (kg)	Sample Worth, (Ih)	Reactivity Coefficient, (Ih/kg)
SS (Type 304)	1.017	-1.50 ± 0.5	-1.47 ± 0.5[a]
Sulphur[b]	0.200	-1.35 ± 0.6	-6.76 ± 3.0
Tungsten[b]	1.867	-14.35 ± 0.6	-7.69 ± 0.3
Thorium	1.5115	-14.75 ± 0.5	-9.76 ± 0.3
Beryllium	0.2407	+22.50 ± 0.5	+93.5 ± 2.0
Polyethylene	0.01453	+17.50 ± 0.5	+1204.0 ± 34

[a]Value for Assembly 31 = 1.4 ± 0.5 Ih/kg.

[b]These samples were canned in stainless steel. The sample mass is that of the named material only. The sample worth has been corrected for the effect of stainless steel.

Table XV

REACTIVITY COEFFICIENTS OF NONFISSILE MATERIALS
AT A RADIUS OF 13.10 IN.

Material	Sample Mass, (kg)	Sample Worth, (Ih)	Reactivity Coefficient (Ih/kg)
SS (Type 304)	1.017	+2.50 ± 0.5	+2.45 ± 0.5
Sulphur[a]	0.200	+0.36 ± 0.6	+1.80 ± 3.0
Tungsten[a]	1.867	-2.75 ± 0.6	-1.47 ± 0.3
Thorium	1.5115	-3.60 ± 0.5	-2.38 ± 0.3

[a]See footnote (b) to Table XIV.

I. Fission Rate Distributions

Fission rate scans along a horizontal radius were made with enriched and depleted uranium fission chambers. One set of scans was made along a radius parallel to the planes of the fuel plates and another set perpendicular to the fuel planes. The main object of the measurements was to detect any appreciable asymmetry of the flux distribution.

In the case of the radial scans parallel to the fuel plates, the columns of fuel in drawers 1-P-16 and 2-P-16 were replaced by 2 rows of $\frac{1}{16}$-in.-thick plates (see Fig. 20).

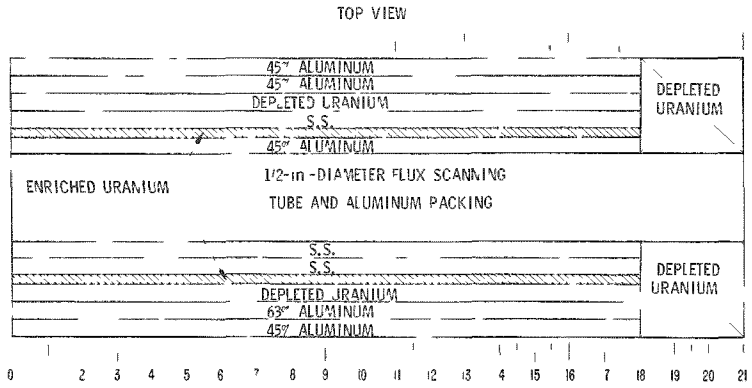

Fig. 20. Drawer Loading for Fission Rate Scan Parallel to Fuel-plate Planes for Assembly 39.

For the scans across the fuel plates, the core material in the row P drawers of Half No. 2 of the reactor was moved back 1 in. and the front of the drawers loaded as shown in Fig. 21. Since measurements with the counter were always about the same distance from a fuel-plate plane, the effects of fine structure were reduced.

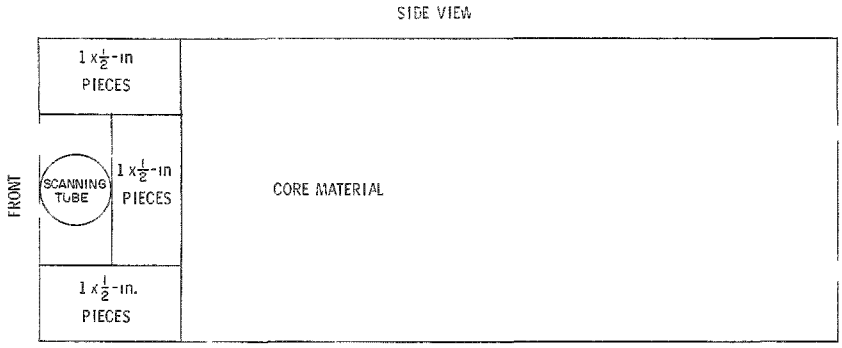

Fig. 21. Drawer Loading for Fission Rate Scan Perpendicular to the Fuel Plates for Assembly 39.

In Tables XVI through XIX the errors quoted are based purely on the counting statistics and represent 66% confidence limits. It is clear that these errors are unrealistic and that errors must arise from some or all of the following:

1. inexact indication of the traverse counter position;
2. instability of the traverse or monitor counter channels;
3. noise pulses;
4. fine-structure effects.

Table XVI

HORIZONTAL RADIAL FISSION RATE DISTRIBUTION FOR ENRICHED URANIUM[a] PARALLEL TO THE FUEL-PLATE PLANES
(Core Radius = 17.9 in.)

Distance from Core Center, (in.)	Relative Fission Rate	Distance from Core Center, (in.)	Relative Fission Rate
0	1.000 ± 0.015[b]	0	1.000 ± 0.015[b]
1	0.998 ± 0.015	-1	0.983 ± 0.015
2	0.997 ± 0.015	-2	0.984 ± 0.015
3	0.979 ± 0.015	-3	0.981 ± 0.015
4	0.960 ± 0.014	-4	0.966 ± 0.014
5	0.939 ± 0.014	-5	0.930 ± 0.014
6	0.919 ± 0.014	-6	0.908 ± 0.014
8	0.829 ± 0.012	-8	0.886 ± 0.013
9	----	-9	----
10	0.786 ± 0.012	-10	0.802 ± 0.012
12	0.697 ± 0.010	-12	0.722 ± 0.011
14	0.645 ± 0.010	-14	0.648 ± 0.010
15	----	-15	0.608 ± 0.009
16	0.517 ± 0.008	-16	0.548 ± 0.008
17	0.478 ± 0.007	-17	0.502 ± 0.007
	----	-17.8	0.476 ± 0.007
18	0.419 ± 0.006		
19	0.335 ± 0.005		
20	0.268 ± 0.004		

(a) 93.2% U^{235}, 6% U^{238}, and 1% U^{234}.

(b) See Paragraph I, Section IV for derivation of errors.

Table XVII

COMPARISON OF HORIZONTAL RADIAL FISSION RATE DISTRIBUTIONS FOR ENRICHED URANIUM[a] PARALLEL AND PERPENDICULAR TO THE FUEL-PLATE PLANES
(Core Radius = 17.9 in.)

Scan Parallel to Fuel		Scan Perpendicular to Fuel	
Distance from Core Center, (in.)	Relative Fission Rate	Distance from Core Center, (in.)	Relative Fission Rate
0.09	1.000 ± 0.004[b]	0	1.000 ± 0.004[b]
-	----	5	0.947 ± 0.004
6.16	0.928 ± 0.004	-	----
-	----	7	0.890 ± 0.004
9.19	0.828 ± 0.003	9	0.833 ± 0.003
12.16	0.725 ± 0.003	12	0.716 ± 0.003
-	----	14	0.619 ± 0.002
17.16	0.495 ± 0.002	17	0.482 ± 0.002
		18	0.429 ± 0.004
		18.5	0.387 ± 0.004
		19.5	0.310 ± 0.003

(a) 93.2% U^{235}, 6% U^{238}, and 1% U^{234}.

(b) See Paragraph I, Section IV for derivation of errors.

Table XVIII

HORIZONTAL RADIAL FISSION RATE DISTRIBUTION FOR DEPLETED URANIUM PARALLEL TO THE FUEL-PLATE PLANES
(Core Radius = 17.9 in.)

Distance from Core Center, (in.)	Relative Fission Rate	Distance from Core Center, (in.)	Relative Fission Rate
0	1.000 ± 0.015*	0	1.000 ± 0.015*
1	1.027 ± 0.015	-1	0.993 ± 0.015
2	1.000 ± 0.015	-2	0.999 ± 0.015
3	0.984 ± 0.015	-3	0.944 ± 0.014
4	0.981 ± 0.015	-4	0.957 ± 0.014
5	0.976 ± 0.015	-5	0.903 ± 0.014
6	0.929 ± 0.014	-6	0.898 ± 0.013
8	0.886 ± 0.013	-	---
10	0.780 ± 0.012	-10	0.785 ± 0.012
12	0.687 ± 0.010	-	---
14	0.574 ± 0.009	-14	0.586 ± 0.009
16	0.429 ± 0.006		
17	0.352 ± 0.005		
18	0.218 ± 0.003		
19	0.136 ± 0.002		
20	0.078 ± 0.001		

* See Paragraph I, Section IV for derivation of errors.

Table XIX

COMPARISON OF HORIZONTAL RADIAL FISSION RATE DISTRIBUTIONS FOR DEPLETED URANIUM PARALLEL AND PERPENDICULAR TO THE FUEL-PLATE PLANES
(Core Radius = 17.9 in.)

Distance from Core Center, (in.)	Scan Parallel to Fuel Relative Fission Rate	Scan Perpendicular to Fuel Relative Fission Rate
0	1.000 ± 0.015*	1.000 ± 0.015*
2	1.000 ± 0.015	0.918 ± 0.009
5	0.940 ± 0.014	0.896 ± 0.009
12	0.687 ± 0.010	0.648 ± 0.006
14	0.574 ± 0.009	0.551 ± 0.006
17	0.352 ± 0.005	0.348 ± 0.003
18	0.218 ± 0.003	0.254 ± 0.003

* See Paragraph I, Section IV for derivation of errors.

An attempt was made to obtain more accurate results for a few positions on each of the enriched uranium scans. For this purpose, a BF_3 counter in the blanket (instead of a much less sensitive fission chamber in the core) was used as a power monitor, and a total of $\approx 10^6$ counts recorded for each position of the traverse counter; about 10^5 counts were recorded on the traverse counter itself. Some positions of the traverse counter corresponding to positions shown on the control room indicator were measured directly before or after a scan.

The results of the more precise scans are given in Table XVII and plotted in Fig. 22. The 2 scans are closely similar; the maximum difference, of about 4%, occurs at the edge of the core. This difference is not accommodated by the quoted errors, but in view of the discrepancy between the quoted and actual errors for the other scans it cannot safely be regarded as real.

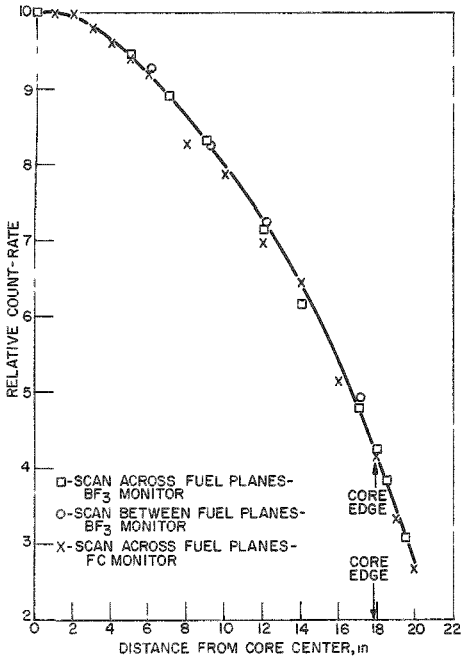

Fig. 22. Horizontal Radial Fission Rate Scans with Enriched (93%) Uranium Parallel and Perpendicular to the Fuel-plate Planes for Assembly 39.

J. Central Fission Ratios

The central neutron spectrum was expected to be essentially unchanged from Assembly 31; hence, only 3 fission chamber measurements were performed as a check on repeatability. The fission chambers, the same 3 which had been used in Assembly 31, were alternately placed in the central spectrum in an identical manner with that used in Assembly 31. The count rates were measured relative to the same U^{235} standard counter.

The results, as given in Table XX, indicate agreement within 1.5%, with no apparent systematic deviation due to the reference counter.

Table XX

COMPARISON OF FISSION COUNTERS IN ASSEMBLIES 31 AND 39

Counter No.	Principal Isotope	Relative Count Rate[a] [Counter "i" (U^{235} Counter)] Assembly 31	Assembly 39	Agreement[a] (31, 39)
16	U^{233}	0.9953 ± 0.71%	0.9961 ± 0.32%	-0.08% ± 0.8%
2	U^{238}	0.02924 ± 0.7%	0.02967 ± 0.5%	-1.45% ± 0.86%
19	Pu^{239}	0.7368 ± 0.63%	0.7274 ± 0.3%	+ 1.3% ± 0.7%

[a] The errors quoted represent 66% statistical confidence (one standard deviation) with respect to the count rates.

K. Summary of Conclusions

1. The critical mass of Assembly 39 was 426.5 kg U^{235} and the shape factor for Assembly 31 was 0.921 ± 0.002.

2. The ratio of the central reactivity coefficients of U^{235} and Pu^{239} for Assemblies 31 and 39 were in agreement.

3. Agreement of the Kirn fission chamber measurements (for U^{233}, U^{238}, and Pu^{239} loaded chambers) for Assemblies 31 and 39 was within 1.5%.

4. No asymmetry of flux distribution, due to heterogeneity of the core, was detected in Assembly 39.

REFERENCES

1. B. C. Cerutti et al., ZPR-III, Argonne's Fast Critical Facility, Nuclear Science and Engineering, 1, 126 (1956).

2. W. B. Loewenstein and G. W. Main, Fast Reactor Shape Factors and Shape Dependent Variables, ANL-6403 (Nov 1961).

3. W. G. Davey and R. N. Curran, An Experimental Investigation of Some Sources of Error in the Measurement of Absolute Fission Ratios in Fast Reactors, ANL-6468 (Nov 1961).

4. J. M. Gasidlo, J. K. Long, and R. L. McVean, Critical Studies of a Dilute Fast Reactor Core, ANL-6338.